Electronic Supplementary Material

Engineering the grain boundary: a promising strategy to configure $NiCoP_4O_{12}$/NiCoP nanowire arrays for ultrastable supercapacitor

Mengqi Cui[1], Zining Wang[1], Yuanye Jiang[1], Hui Wang (✉)[1,2]

1 State Key Laboratory Base for Eco-Chemical Engineering, College of Chemical Engineering, Qingdao University of Science and Technology, Qingdao 266042, China

2 Guangdong Provincial Key Laboratory for Electronic Functional Materials and Devices, Huizhou University, Huizhou 516001, China

Physical characterization

Crystal structure of as-prepared samples was investigated by X-ray diffraction(XRD) on a Shimadzu XD-3A instrument, and XRD patterns were recorded by Cu- Kα radiation with λ=0.15418 nm. The 2θ scan rate of XRD analysis was set at 10 min^{-1}. The average crystal size of the samples was calculated by Debye-Scheler's formular.

$B_{2\theta} = 0.94\lambda/L\cos\theta$

$B_{2\theta}$- width of half peak

λ- incident wave length

L-particle diameter

θ-diffraction angle

Based on the (311) plane of $NiCo_2O_4$ and the (111) plane of NiCoP, the histogram graph of calculated average crystal size are presented in Figure 2h. Their microstructure was investigated on a Carl Zeiss scanning electron microscope and a JEOL (JEM-2000 FX) transmission electron microscope. High angle annular dark field scanning transmission electron microscopy (STEM) of the catalysts were done by the same JEOL instrument operating at 200 kV. X-ray photoelectron spectroscopy (XPS) was carried out on a PHI-5702 spectrometer and C1 s peak at 285.0 eV was used as a reference for binding energies calibration.

Electrochemical measurements

Electrochemical performance of as-prepared NiCoP was studied using a CHI 660E electrochemical workstation. The experiments were carried out in a three-electrode configuration with a 1×1 cm^2 sample, activated carbon (AC) and Hg/HgO (1.0 M KOH) serving as working electrode, counter electrode and reference electrode respectively. Cyclic voltammetry (CV) graphs were recorded in a three- and a two-electrode systems in 1 M KOH aqueous electrolytes. Galvanostatic charge/discharge (GCD) and cycling tests were conducted using a LAND CT2001A battery measurement system. Areal specific capacity (C_a), energy density (E) and power density (P) were calculated according to the following equations:

$$C_a = 2I \times \int V\, dt / (A \times V) \qquad (1)$$

$$E = C_m \times (\Delta V)^2 / 2 \qquad (2)$$

$$P = E / \Delta t \qquad (3)$$

where I, t, m, ΔV, and A represent discharge current (mA), discharge time (s), total mass of active materials (g), electrode potential window (V), and electrode surface area (cm^2) respectively.

Prior to assembly of the asymmetric supercapacitor, mass loadings of both cathode and anode were balanced according to the following equation:

$$m^+/m^- = C^- \times \Delta E^- / (C^+ \times \Delta E^+) \qquad (4)$$

where mass ratio of cathode to anode particles was set at 0.3.

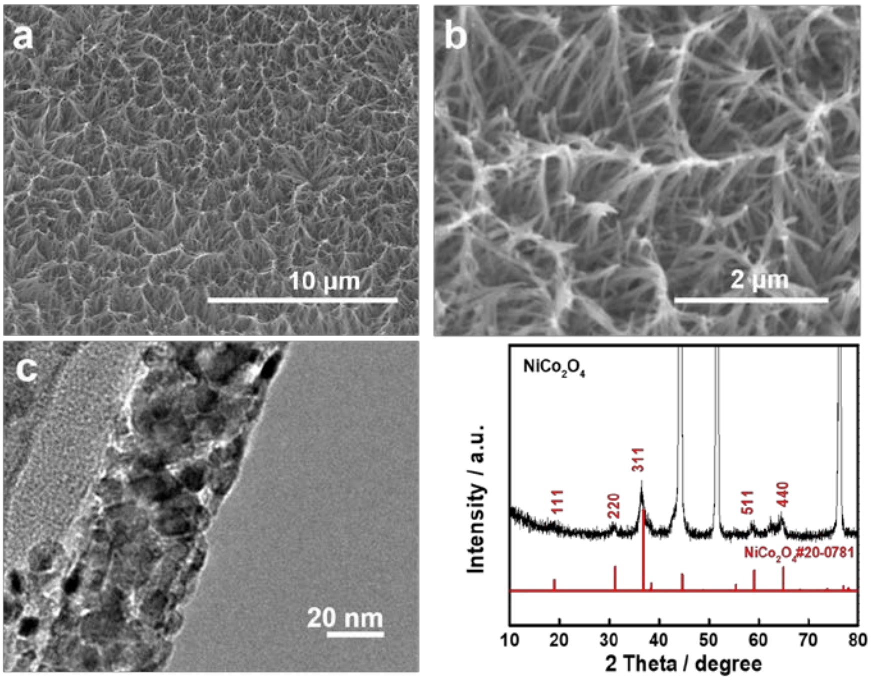

Figure. S1 (a, b) SEM, (c) TEM and (d) XRD of $NiCo_2O_4$ rods.

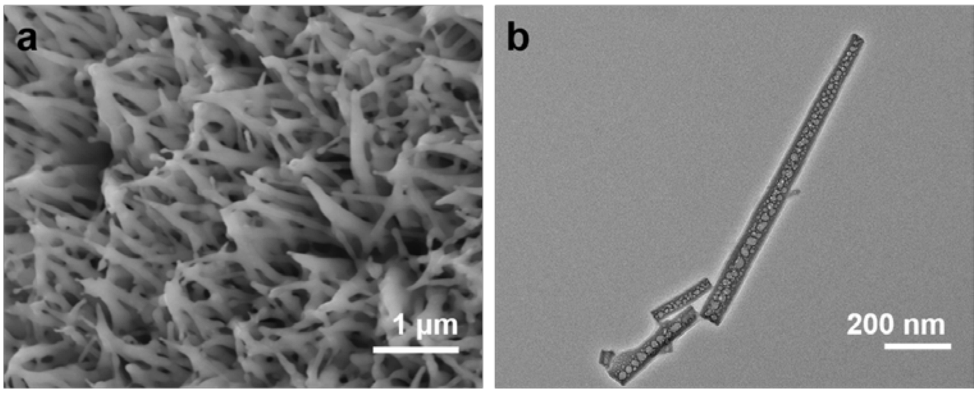

Figure. S2 (a)SEM images and (b) TEM images of the $NiCoP_4O_{12}$/NiCoP-30 sample.

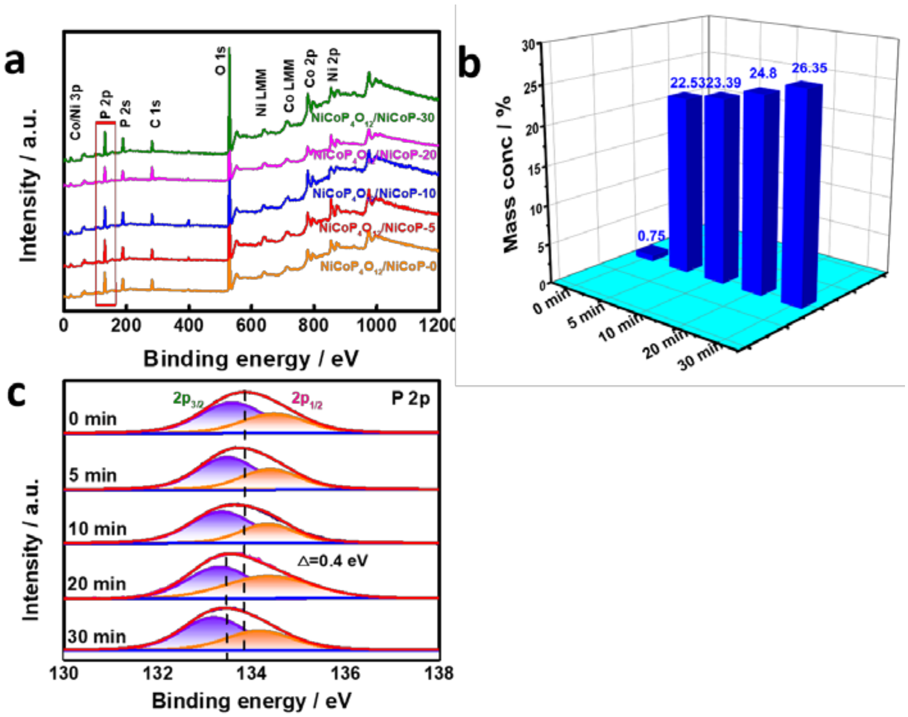

Figure. S3 (a) XPS survey spectrum, (b) P atomic content based on the integral area from a, and (c) the fitted P 2p XPS of the all samples.

In the high-resolution P 2p XPS spectra of the $NiCoP_4O_{12}$/NiCoP samples in Figure S3c, two peaks at 133.6 and 134.4 eV of binding energy correspond to $2p_{1/2}$ and $2p_{3/2}$ of P 2p, respectively, which suggests the P atoms in the $NiCoP_4O_{12}$/NiCoP samples are in oxidation state. As a result of the decreased content of the high-valence oxidation state of P atoms, the binding energies from sample $NiCoP_4O_{12}$/NiCoP-0 to $NiCoP_4O_{12}$/NiCoP-30 shift back about 0.4 eV, and the decrease of $NiCoP_4O_{12}$ has been proved by XRD.

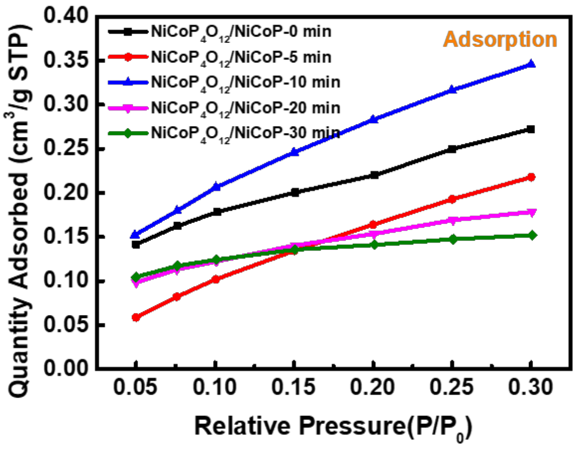

Figure. S4 N_2 adsorption isotherm of the samples.

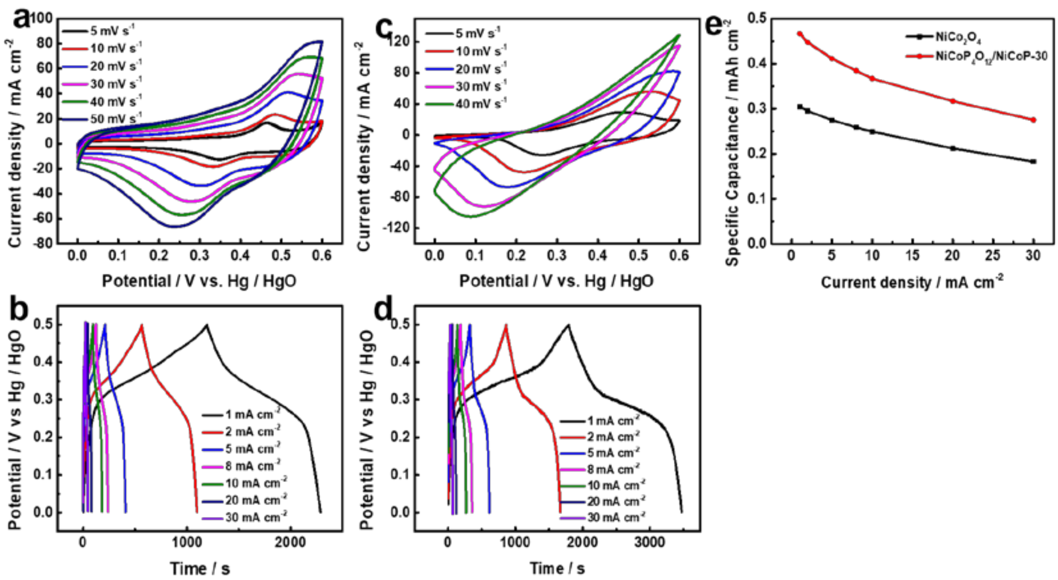

Figure. S5 (a) CV curves of $NiCo_2O_4$ at various scan rates; (b) GCD curves of $NiCo_2O_4$ at different current densities; (c) CV curves of $NiCoP_4O_{12}$/NiCoP-30 at various scan rates; (d) GCD curves of $NiCoP_4O_{12}$/NiCoP-30 at different current densities; (e) Specific capacitance *vs.* current density for the $NiCo_2O_4$ and $NiCoP_4O_{12}$/NiCoP-30 samples.

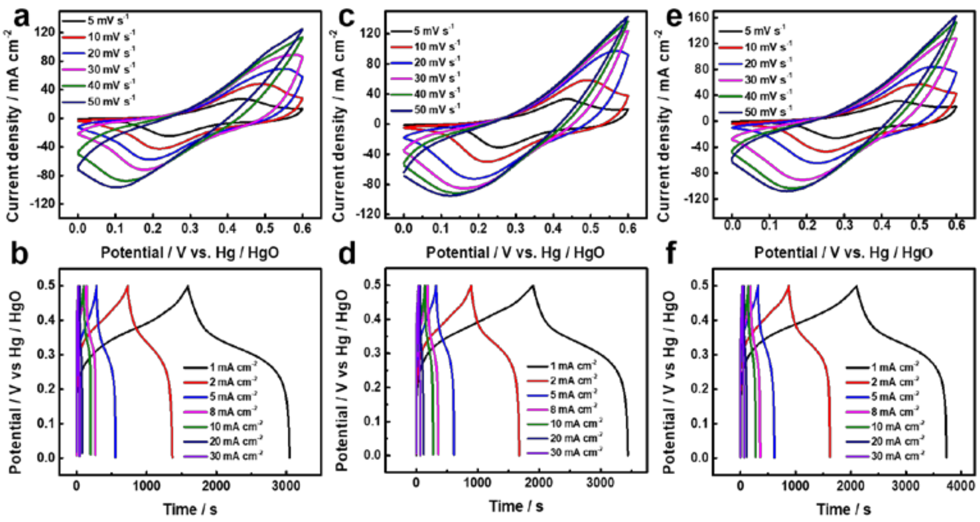

Figure. S6 (a) and (b) CV and GCD of the $NiCoP_4O_{12}$/NiCoP-0 min respectively; (c) and (d) CV and GCD of the $NiCoP_4O_{12}$/NiCoP-5 min respectively; (e) and (f) CV and GCD of the $NiCoP_4O_{12}$/NiCoP-20 min respectively.

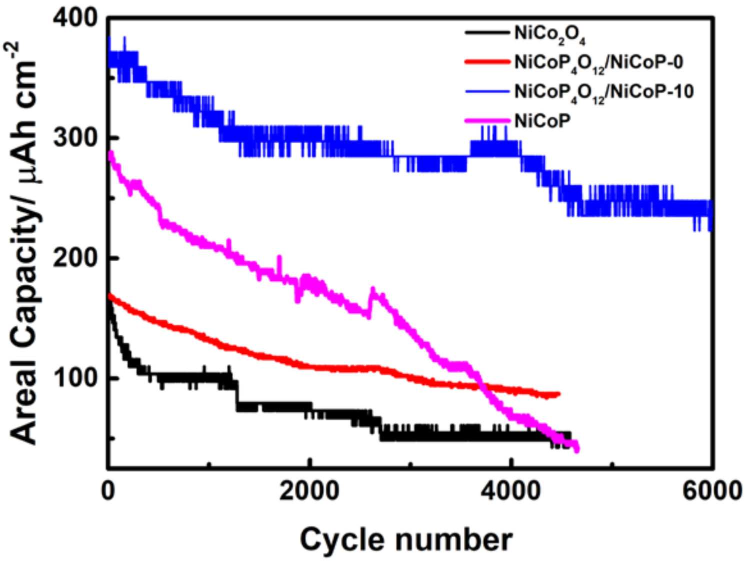

Figure. S7 Three-electrode cycling stability test of different samples at 30 mA cm^{-2}.

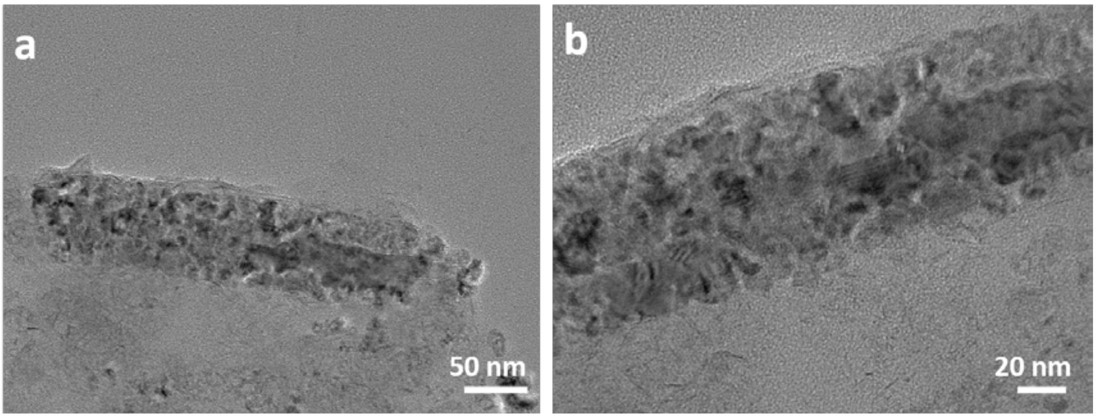

Figure. S8 TEM image of sample after cycling stability.

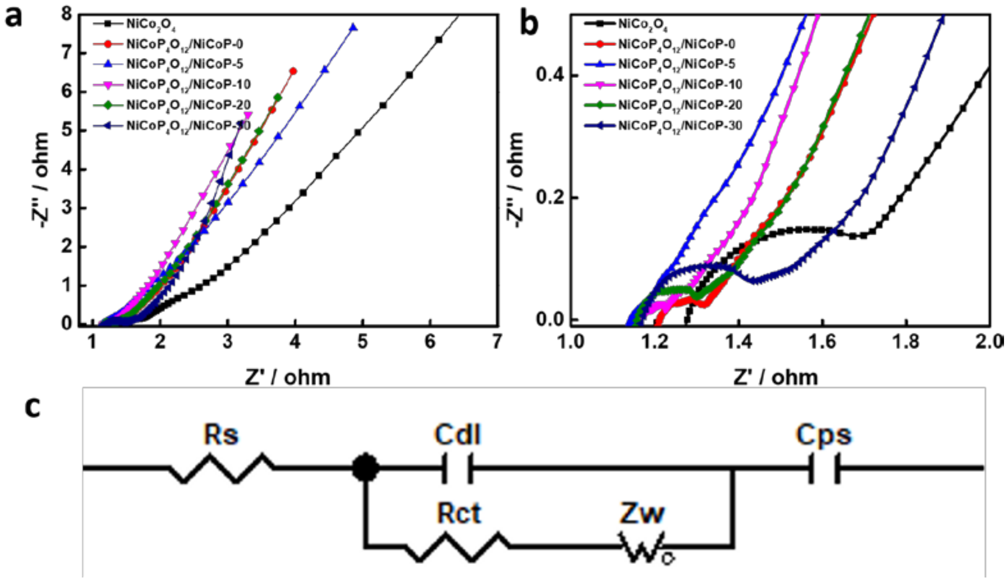

Figure. S9 a and b are the EIS diagrams of the samplea, and c is the equivalent circuit diagram of the sample.

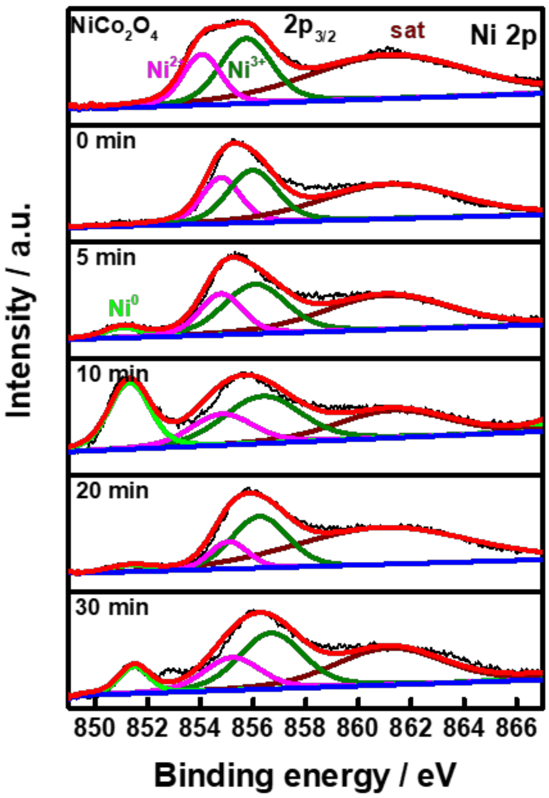

Figure. S10 The fitted Ni 2p XPS spectra of the samples.

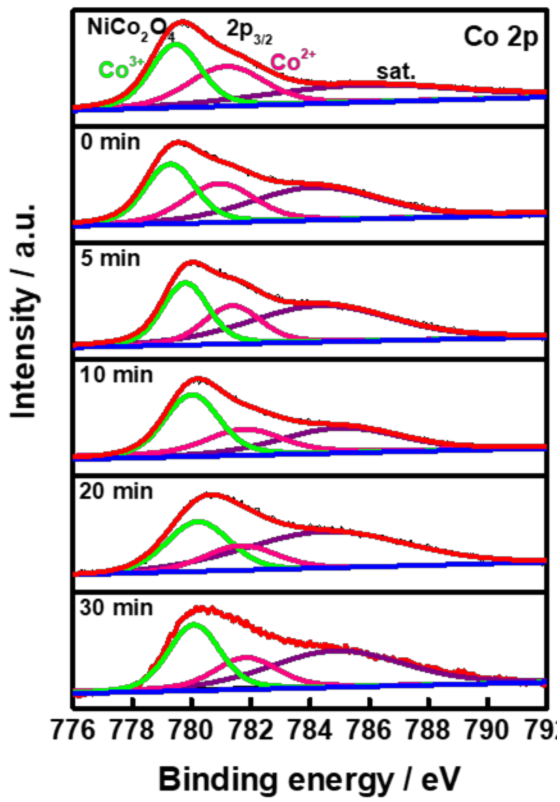

Figure. S11 The fitted Co 2p XPS spectra of the samples.

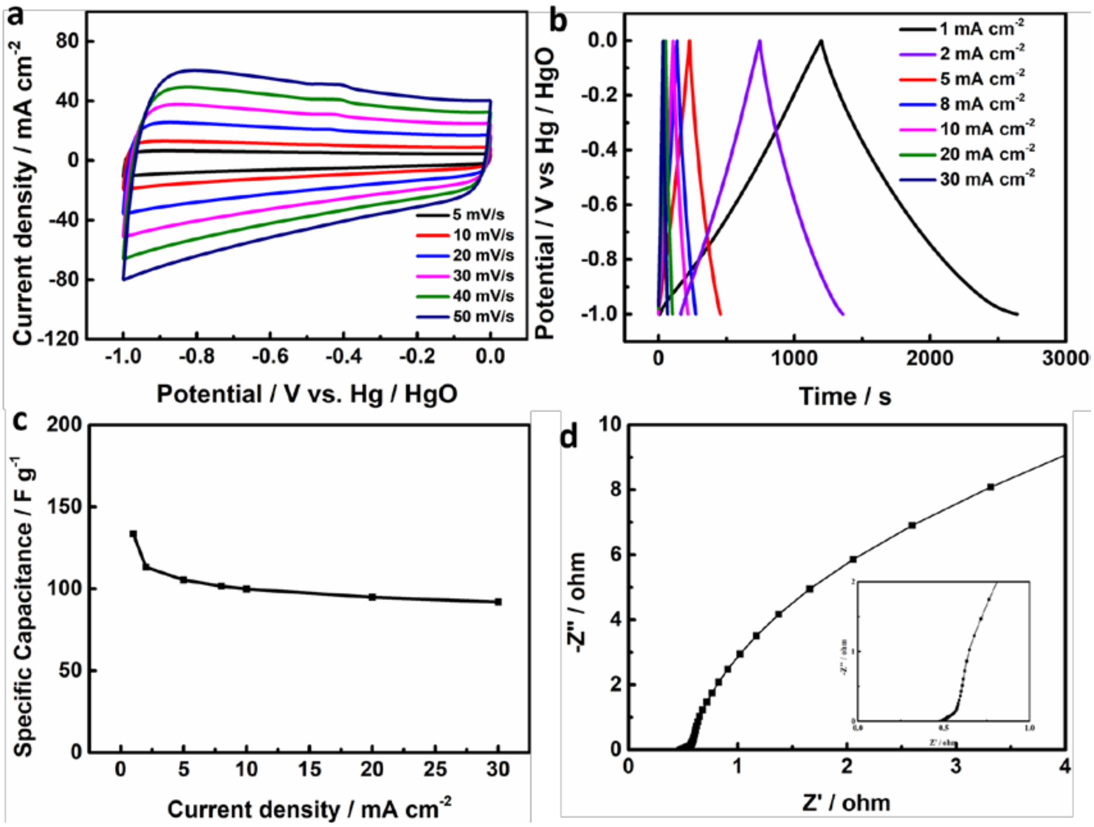

Figure. S12 a) CV curves of activated carbon anode at various scan rates; b) GCD for activated carbon anode EIS responses obtained for activated carbon anode; c) Specific capacity from GCD for activated carbon anode; d) EIS responses obtained for activated carbon anode.

Table S1 The fitted impedance from EIS of all the samples.

Samples	Rct(ohm)	Zw(ohm)
$NiCo_2O_4$	0.999949	1.601
$NiCoP_4O_{12}$/NiCoP -0	0.98242	1.447
$NiCoP_4O_{12}$/NiCoP-5	0.99388	0.91539
$NiCoP_4O_{12}$/NiCoP-10	1.003	0.77289
$NiCoP_4O_{12}$/NiCoP-20	1.01	0.77301
$NiCoP_4O_{12}$/NiCoP-30	1.012	0.77363

Table S2 The conductivity of the samples.

Sample	**Square resistance (mΩ)**	**Conductivity (KS/mm)**
$NiCo_2O_4$	6.05495	0.10898
$NiCoP_4O_{12}$/NiCoP-0	6.00683	0.11193
$NiCoP_4O_{12}$/NiCoP-5	5.93956	0.11359
$NiCoP_4O_{12}$/NiCoP-10	5.41784	0.12432
$NiCoP_4O_{12}$/NiCoP-20	5.54320	0.12196
$NiCoP_4O_{12}$/NiCoP-30	5.65451	0.11907

Table S3 The binding energy of the fitted Ni species of the samples.

Sample	Binding energy and atomic percentage of Ni species (eV/%)		
	Ni(+2)	Ni(+3)	Ni(0)
$NiCo_2O_4$	854.0/31.16%	855.7/68.84%	---
$NiCoP_4O_{12}$/NiCoP-0	854.7/30.68%	855.9/69.32%	---
$NiCoP_4O_{12}$/NiCoP-5	854.8/25.41%	856.1/66.58%	851.0/8.01%
$NiCoP_4O_{12}$/NiCoP-10	854.8/15.57%	856.4/40.98%	851.2/43.45%
$NiCoP_4O_{12}$/NiCoP-20	855.1/24.60%	856.2/68.14%	851.3/7.26%
$NiCoP_4O_{12}$/NiCoP-30	855.1/23.73%	856.7/67.76%	851.4/8.51%

Table S4 The binding energy of the fitted Co species of the samples.

Sample	Binding energy and atomic percentage of Co species (eV/%)	
	Co(+2)	Co(+3)
$NiCo_2O_4$	781.1/50.29%	779.4/49.71%
$NiCoP_4O_{12}$/NiCoP-0	781.1/47.99%	779.4/52.01%
$NiCoP_4O_{12}$/NiCoP-5	781.3/46.18%	779.7/53.82%
$NiCoP_4O_{12}$/NiCoP-10	781.7/40.17%	779.9/59.83%
$NiCoP_4O_{12}$/NiCoP-20	781.7/36.85%	780.1/63.15%
$NiCoP_4O_{12}$/NiCoP-30	781.8/36.4%	780.1/63.6%

Table S5 Comparison of cycle stability of the different samples.

Samples	**Stability**	**Ref**
$NiCoP_4O_{12}$/NiCoP	88.5%(10000 cycles)	This work
NiCoP/$Co(OH)_2$	87%(6000 cycles)	[1]
NiP@NiCo LDH//AC	70% (5000 cycles)	[2]
NiCoP//AC	67.2% (5000 cycles)	[3]
$Ni_xCo_{1-x}O/NiyCo_{2-y}P$@C//AC	75% (7000 cycles)	[4]
NiCoP/CoP	87% (10000 cycles)	[5]
NiCoP/CNT	85% (5000 cycles.)	[6]

References

1. Wang H, Zhu Y, Zong Q, Wang Q, Yang H, Zhang Q. Hierarchical NiCoP/Co(OH)$_2$ nanoarrays for high-performance asymmetric hybrid supercapacitors. Electrochimica Acta, 2019, 321: 134746.

2. Xing J, Du J, Zhang X, Shao Y, Zhang T, Xu C. A Ni-P@NiCo LDH core-shell nanorod-decorated nickel foam with enhanced areal specific capacitance for high-performance supercapacitors. Dalton Trans, 2017, 46(30): 10064-10072

3. Lan Y, Zhao H, Zong Y, Li X, Sun Y, Feng J, Wang Y, Zheng X, Du Y. Phosphorization boosts the capacitance of mixed metal nanosheet arrays for high performance supercapacitor electrodes. Nanoscale, 2018, 10(25): 11775-11781

4. Shao Y, Zhao, Li H, Xu C. Three-dimensional hierarchical $Ni_xCo_{1-x}O/Ni_yCo_{2-y}P$@C hybrids on Nickel foam for excellent supercapacitors. ACS Applied Materials & Interfaces, 2016, 8(51): 35368-35376

5. Dang T, Wei D, Zhang G, Wang L, Li Q, Liu H, Cao Z, Zhang G, Duan H. Homologous NiCoP/CoP hetero-nanosheets supported on N-doped carbon nanotubes for high-rate hybrid supercapacitors. Electrochimica Acta, 2020, 341: 135988

6. Zhao G, Tang Y, Wan G, Xu X, Zhou X, Zhou M, Hao C, Deng S, Wang G. High-performance and flexible all-solid-state hybrid supercapacitor constructed by NiCoP/CNT and N-doped carbon coated CNT nanoarrays. Journal of Colloid and Interface Science, 2020, 572: 151-159